

## Low-decoherence flux qubit

J. Q. You,<sup>1,2</sup> Xuedong Hu,<sup>3</sup> S. Ashhab,<sup>2</sup> and Franco Nori<sup>2,4</sup>

<sup>1</sup>Department of Physics and Surface Physics Laboratory (National Key Laboratory), Fudan University, Shanghai 200433, China

<sup>2</sup>Frontier Research System, The Institute of Physical and Chemical Research (RIKEN), Wako-shi 351-0198, Japan

<sup>3</sup>Department of Physics, University at Buffalo, SUNY, Buffalo, New York 14260-1500, USA

<sup>4</sup>Center for Theoretical Physics, Physics Department, Center for the Study of Complex Systems, University of Michigan, Ann Arbor, Michigan 48109-1040, USA

(Received 3 April 2007; published 27 April 2007)

A flux qubit can have a relatively long decoherence time at the degeneracy point, but away from this point the decoherence time is greatly reduced by dephasing. This limits the practical applications of flux qubits. Here we propose a qubit design modified from the commonly used flux qubit by introducing an additional capacitor shunted in parallel to the smaller Josephson junction (JJ) in the loop. Our results show that the effects of noise can be considerably suppressed, particularly away from the degeneracy point, by both reducing the coupling energy of the JJ and increasing the shunt capacitance. This shunt capacitance provides a novel way to improve the qubit.

DOI: 10.1103/PhysRevB.75.140515

PACS number(s): 03.67.Pp, 03.65.Yz, 03.67.Lx, 85.25.-j

Superconducting quantum circuits based on Josephson junctions (JJs) are promising candidates of qubits for scalable quantum computing (see, e.g., Ref. 1). Like other types of superconducting qubits, flux qubits have been shown to have quantum-coherent properties (see, e.g., Refs. 2–8). A recent experiment<sup>7</sup> showed that this qubit has a long decoherence time  $T_2$  ( $\sim 120$  ns) at the degeneracy point; this  $T_2$  can become as long as  $\sim 4$   $\mu$ s by means of spin-echo techniques. However, even *slightly away* from the degeneracy point, the decoherence time is drastically reduced. This sensitivity to flux bias considerably limits the applications both for flux qubits for quantum computing and also when performing quantum-optics and atomic-physics experiments on microelectronic chips with the qubit as an artificial atom.

Typically, JJ circuits have two energy scales: the charging energy  $E_c$  of the JJ and the Josephson coupling energy  $E_J$  of the junction. Ordinarily, a flux qubit works in the phase regime with  $E_J/E_c \gg 1$ , where its decoherence is dominated by flux fluctuations. For the widely used three-junction flux qubit design,<sup>2–6</sup> in addition to two identical JJs with coupling energy  $E_J$  and charging energy  $E_c$ , a third JJ, which has an area smaller by a factor  $\alpha \sim 0.7$ , is employed to properly adjust the qubit spectrum. Charge fluctuations can affect the decoherence of this flux qubit via the smaller junction.

Here we search for an improved design for flux qubits. We show that reducing the ratio  $E_J/E_c$  suppresses the effects of flux noise, although charge noise becomes increasingly important. Reducing  $\alpha$  further suppresses the effects of flux noise and considerably improves the decoherence properties away from the degeneracy point. As the effect of flux noise has been largely suppressed, charge noise would now be the dominant source of decoherence. It mainly comes from the charge fluctuations on the two islands separated by the smaller JJ and affects the qubit mainly through relaxation. We thus propose an improved flux qubit by introducing a large capacitor that shunts in parallel to the smaller JJ. This shunt capacitance suppresses the effects of the dominant charge noise in the two islands separated by the smaller JJ by reducing the charging energy. Our results reveal that using a

larger shunt capacitor allows reducing both  $E_J/E_c$  and  $\alpha$  to considerably suppress the effects of both flux and charge noises, particularly away from the degeneracy point. In essence, our method reduces the couplings of the flux qubit to the *two* types of noise. It provides a promising approach for lowering the decoherence of JJ qubits.

We consider, as a typical example, a modified version of the usual three-junction flux qubit;<sup>2–6</sup> it consists of a superconducting loop containing three JJs and pierced by a magnetic flux. The new ingredient, which drastically improves the qubit, is an additional capacitance  $C_s$  shunted in parallel to the smaller JJ (Fig. 1). Note that our approach also applies to flux qubits with any number of junctions—e.g., the four-junction design—by shunting a capacitor to the smaller junction. As shown in Fig. 1, the three JJs divide the superconducting loop into three islands, denoted by  $a$ ,  $b$ , and  $c$ . When

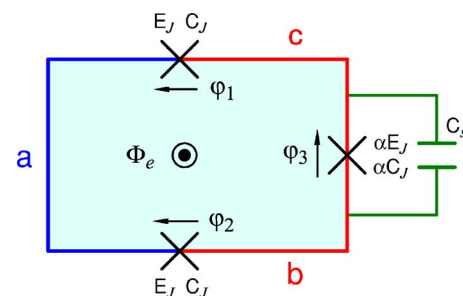


FIG. 1. (Color online) (a) Schematic of a low-decoherence flux qubit. The loop is pierced by an externally applied magnetic flux  $\Phi_e$  and interrupted by three Josephson junctions (JJs) that divide the loop into three islands denoted by  $a$  (blue),  $b$  (red), and  $c$  (red). The two identical JJs have coupling energy  $E_J$  and capacitance  $C_J$ , while the third (smaller) JJ has coupling energy  $\alpha E_J$  and capacitance  $\alpha C_J$ , where  $0.5 < \alpha < 1$ . Here a capacitance  $C_s$  is shunted in parallel to the smaller JJ, so as to reduce the charging energy related to islands  $b$  and  $c$ . The shunt capacitor can be fabricated by depositing a metallic plate below or above the smaller junction, with a dielectric layer between the metallic plate and  $b$  as well as between the plate and  $c$ .

the environment-induced charges on the three islands are taken into account, the Hamiltonian of the system is  $H = E_p(n_p - \delta N_a)^2 + E_m[n_m - (\delta N_b - \delta N_c)]^2 + U(\varphi_p, \varphi_m)$ , where  $n_k = -i\partial/\partial\varphi_k$  ( $k=p, m$ ),  $E_p = 2E_c$ , and  $E_m = E_p/(1+2\beta)$ , with  $E_c = e^2/2C_J$  and  $\beta = \alpha + C_s/C_J$ . Here  $E_p$  is the charging energy of the island  $a$ ,  $E_m$  is the effective charging energy related to islands  $b$  and  $c$ , and  $\delta N_i$  ( $i=a, b$ , and  $c$ ) are the environment-induced charges (in units of  $2e$ ) on the islands. The potential energy is  $U(\varphi_p, \varphi_m) = 2E_J(1 - \cos\varphi_p \cos\varphi_m) + \alpha E_J[1 - \cos(2\pi f + 2\varphi_m)]$ , where  $\varphi_p = (\varphi_1 + \varphi_2)/2$  and  $\varphi_m = (\varphi_1 - \varphi_2)/2$ . The reduced flux  $f$  is given by  $f = f_e + \delta f$ , with  $f_e = \Phi_e/\Phi_0$  and  $\delta f = \delta\Phi/\Phi_0$ , where  $\Phi_e$  is the externally applied magnetic flux in the loop,  $\delta\Phi$  the flux fluctuations, and  $\Phi_0 = h/2e$ .

We study the environment-induced effects on the qubit by expanding the Hamiltonian  $H$  into a series and truncating it to keep the interaction terms to lowest order. Including the environmental Hamiltonian  $H_{\text{env}}$ , we can write the total Hamiltonian  $H_t$  as  $H_t = H_q + H_{\text{env}} + H_{\text{int}}$ , where  $H_q = H(\delta N_i = 0, \delta f = 0)$  is the Hamiltonian of the qubit and the interaction Hamiltonian takes the form  $H_{\text{int}} = -2E_p n_p \delta N_a - 2E_m n_m (\delta N_b - \delta N_c) - I\Phi_0 \delta f$ , where  $I = -\alpha I_c \sin(2\pi f_e + 2\varphi_m)$  with  $I_c = 2\pi E_J/\Phi_0$ .

To study the coherence properties of this flux qubit, we project the total Hamiltonian onto the subspace spanned by the qubit eigenstates  $|0\rangle$  and  $|1\rangle$  with eigenenergies  $E_0$  and  $E_1$ , the two lowest energy levels of the quantum device. Now the flux-qubit Hamiltonian is reduced to  $H_q = \frac{1}{2}\varepsilon\sigma_z$ , with  $\varepsilon = E_1 - E_0$  and  $\sigma_z = |1\rangle\langle 1| - |0\rangle\langle 0|$ , while the interaction Hamiltonian is reduced to

$$H_{\text{int}} = - \sum_i [\sigma_z X_i - (\sigma_+ Y_i + \text{H.c.})], \quad (1)$$

with  $\sigma_+ = |1\rangle\langle 0|$ . Here the longitudinal couplings  $X_i$ ,  $i=f, a, b$ , and  $c$ , are  $X_i(t) = A_i \delta\lambda_i(t)$ , with  $A_f = \frac{1}{2}\Phi_0(\langle 1|I|1\rangle - \langle 0|I|0\rangle)$ ,  $A_a = E_p(\langle 1|n_p|1\rangle - \langle 0|n_p|0\rangle)$ , and  $A_b = -A_c = E_m(\langle 1|n_m|1\rangle - \langle 0|n_m|0\rangle)$ . The transverse couplings  $Y_i$  are  $Y_i(t) = B_i \delta\lambda_i(t)$ , where  $B_f = \Phi_0\langle 1|I|0\rangle$ ,  $B_a = 2E_p\langle 1|n_p|0\rangle$ , and  $B_b = -B_c = 2E_m\langle 1|n_m|0\rangle$ . The fluctuations are  $\delta\lambda_f \equiv \delta f$  for the flux noise and  $\delta\lambda_i \equiv \delta N_i$  ( $i=a, b$ , and  $c$ ) for the charge noises related to the three islands. The longitudinal coupling term  $\sigma_z X_i$  leads to pure dephasing between the qubit states, while the transverse coupling term  $\sigma_+ Y_i + \text{H.c.}$  leads to relaxation. One way to suppress decoherence from *both* pure dephasing and relaxation is to reduce the longitudinal and transverse couplings by decreasing  $|A_i|$  and  $|B_i|$ . This general method of decoherence suppression applies *irrespective* of the particular behavior of  $\lambda_i(t)$ —i.e., whether it is Gaussian or non-Gaussian noise.

We first study the conventional three-junction flux qubit, without the shunt capacitance  $C_s$ . We take  $\alpha = \beta = 0.8$ , as in the experiment in Ref. 3. Figures 2(a)–2(c) show the flux dependence of the energy levels. The lowest two levels around the degeneracy point  $f_e \equiv \Phi_e/\Phi_0 = 0.5$  are employed as the qubit states. To characterize the effects of the flux noise on this qubit, we introduce longitudinal and transverse coupling strengths defined by  $F_z = |A_f|^2$  and  $F_x = |B_f|^2$ , respectively. To compare the contributions of charge noise with flux

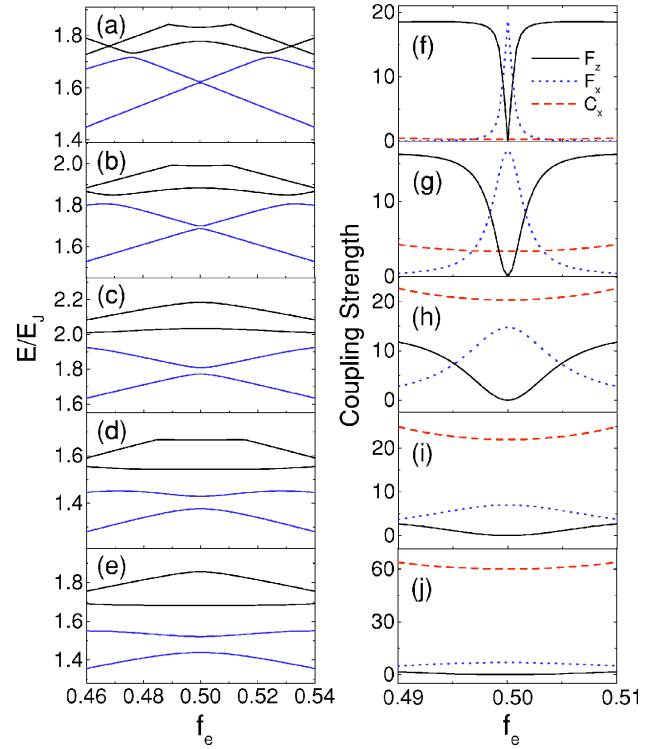


FIG. 2. (Color online) (a)–(e) Energy levels of the flux qubit versus the reduced magnetic flux  $f_e = \Phi_e/\Phi_0$  for  $\alpha = \beta = 0.8$  and  $E_J/E_c =$  (a) 60, (b) 35, and (c) 20 as well as  $\alpha = \beta = 0.6$  and  $E_J/E_c =$  (d) 60 and (e) 35. Here only the lowest four energy levels are shown. (f)–(j) Coupling strength (in units of  $E_J^2$ ) versus the reduced flux  $f_e$ , which corresponds to (a)–(e), respectively. In this figure and the following one, other coupling strength parameters for charge noise are not shown because they are orders of magnitude smaller.

noise, we define the longitudinal and transverse coupling strengths  $C_{zi} = \kappa_i |A_i|^2$  and  $C_{xi} = \kappa_i |B_i|^2$  for the charge noise, where  $i=a, b$ , and  $c$ . The coefficient  $\kappa_i$  characterizes the relative contribution of each charge noise and is defined as  $\kappa_i = S_i(\omega)/S_f(\omega)$ —i.e., the ratio between the power spectra of each charge noise and the flux noise. This definition is reasonable as the qubit relaxation rate is proportional to both  $|B_i|^2$  and the power spectrum of the noise, as shown below [see Eq. (2)]. We estimate  $\kappa_i$  by considering the  $1/f$  noise with power spectrum  $K_i/|\omega|$ . Here  $K_i$  is determined from experiments. Typically,  $K_{\text{charge}} = (0.3 \times 10^{-3})^2$  for the charge noise<sup>9</sup> and  $K_{\text{flux}} = 3 \times 10^{-12}$  for the flux noise.<sup>7</sup> For simplicity, the same  $K_{\text{charge}}$  is used for the three charge noises related to the islands  $a, b$ , and  $c$ , so that  $\kappa_i = K_{\text{charge}}/K_{\text{flux}} \equiv \kappa$ .

In Figs. 2(f)–2(h), we show the flux dependence of the coupling strengths  $F_z$ ,  $F_x$ , and  $C_x$ . At  $f_e = 0.5$ ,  $F_z$  falls to zero, while  $F_x$  rises to its peak. This implies that, at the degeneracy point  $f_e = 0.5$ , the first-order pure dephasing due to flux noise disappears and the flux qubit decoherence is dominated by relaxation. However, for a large  $E_J/E_c$  [see, e.g., Fig. 2(f)], pure dephasing dominates when  $f_e$  is slightly away from the degeneracy point. For decreasing  $E_J/E_c$ , the valley of  $F_z$  around  $f_e = 0.5$  becomes broader, while the peak of  $F_x$  becomes less sharp and its height is gradually reduced. In Figs. 2(f)–2(h) we also show the dominant  $C_{xb} = C_{xc} \equiv C_x$  curves

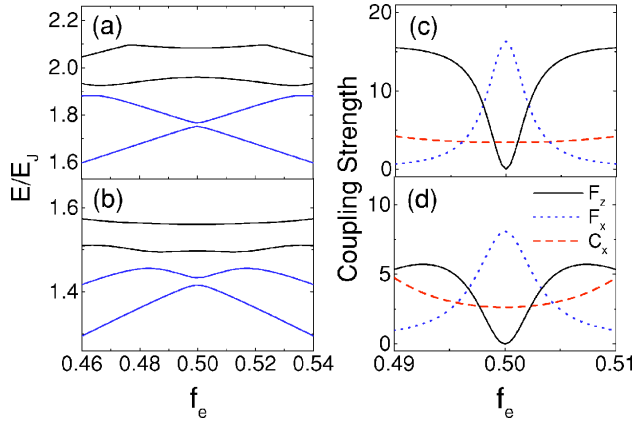


FIG. 3. (Color online) (a) and (b) Energy levels of the flux qubit versus the reduced magnetic flux  $f_e$ . Here, (a)  $\alpha=0.8$ ,  $\beta=1.5$ , and  $E_J/E_c=20$  and (b)  $\alpha=0.6$ ,  $\beta=4$ , and  $E_J/E_c=35$ . (c) and (d) Coupling strength (in units of  $E_J^2$ ) versus the reduced flux  $f_e$ , which correspond to (a) and (b), respectively.

due to charge fluctuations on the smaller islands  $b$  and  $c$ . The quantity  $C_x$  characterizes qubit relaxation induced by charge noise and should be compared to the  $F_x$  curves in the figures. Notice that when  $E_J/E_c$  decreases, charge noise plays an increasingly important role and eventually is more important than flux noise in terms of relaxation [compare the dashed and dotted curves in Fig. 2(h)]. We note here that as shown in Ref. 2, the energy levels of the flux qubit are very flat versus the offset charges. This insensitivity of the energy splittings to the charge fluctuations implies a very weak pure dephasing caused by charge noise. Indeed, we numerically calculated the longitudinal coupling strengths  $C_{za}$  and  $C_{zb} = C_{zc} \equiv C_z$  for our system and found that these quantities are orders of magnitude smaller than  $C_x$ . These results further reveal that the charge-noise-induced dephasing is weak.

Now we reduce the size of the smaller JJ in the conventional 3JJ flux qubit to  $\alpha=\beta=0.6$ . We also show the flux dependence of the energy levels [Figs. 2(d) and 2(e)] and the coupling strengths [Figs. 2(i) and 2(j)]. Here the coupling strengths  $F_z$  and  $F_x$  are reduced and become flatter around  $f_e=0.5$ . This reduction of the flux-noise effects is due to the decrease of the circulating current  $I$  with  $\alpha$ . However, the coupling strength  $C_x$  becomes much larger than  $F_z$  and  $F_x$  because the effects of charge noise are strengthened due to the increase of both charging energy  $E_m$  and transition matrix element  $|\langle 1|n_m|0\rangle|$ . The results here reveal that the *decoherence* of the flux qubit is *sensitive* to the values of  $\alpha$  and  $\beta$  of the small JJ (here  $\alpha=\beta$ ). Moreover, the coupling strength  $C_x$  increases rapidly with decreasing  $E_J/E_c$  [see the dashed curves in Figs. 2(i) and 2(j)]. In short, decreasing  $\alpha$  reduces the coupling strength between the flux qubit and the flux environment, and makes the coupling strength less sensitive to the flux bias so that pure dephasing becomes less important near the degeneracy point. However, decreasing  $\alpha$  also leads to a dramatic increase in the coupling strength between the flux qubit and its charge environment, to the degree that it may become the dominant decoherence channel.

To achieve an improved flux qubit in which the effects of both charge and flux noises are reduced significantly, we

shunt a large capacitance in parallel to the smaller JJ (see Fig. 1) so as to decrease the charging energy  $E_m$  while keeping the ratio  $\alpha$  small. In Fig. 3 we present two examples in which the effects of the charge noise are reduced. In both cases, a small and flat  $C_x$  is achieved. Also, we show that the coupling strengths  $F_z$  and  $F_x$  are smaller and flatter in Fig. 3(d) than in Fig. 3(c). These results indicate that for a suitably chosen  $E_J/E_c$  ratio, by optimally decreasing  $\alpha$  and increasing  $\beta$  one can reduce the coupling of the qubit to *both* flux and charge noises, so that pure dephasing can be considerably reduced in a *wide region* around the degeneracy point  $f_e=0.5$  and the relaxation is significantly suppressed. This corresponds to an improved flux qubit with low decoherence.

Note that the parameter  $\alpha$  has a lower bound of 0.5 for the flux qubit; when  $\alpha<0.5$ , the double-well potential reverts back to a single-well potential and the circuit behaves like a phase qubit. Also, the shunt capacitance should have an upper bound when other factors are taken into account. For instance, a very large shunt capacitance needs a thicker dielectric insulator for fabricating the external capacitor. In this case, the decoherence originating from phonon radiation<sup>10</sup> and defects in the thicker insulator<sup>11</sup> may play more important roles. Furthermore, when the shunt capacitance increases, the energy gap  $\Delta$  of the qubit at the degeneracy point narrows down, raising the single-qubit operation time  $\hbar/\Delta$ . This decrease in  $\Delta$  is another factor one needs to consider in determining the upper bound of the shunt capacitance. One should keep in mind here that reducing  $\alpha$  increases  $\Delta$ . As a result, with properly chosen values of  $\alpha$  and  $\beta$ , the gap  $\Delta$  is not necessarily decreased in the optimized design, as we shall show with an example below.

Finally, we discuss the relation between the decoherence rate and our defined coupling strengths. When each transverse coupling term in Eq. (1) is treated as a perturbation, according to the Fermi golden rule, one can obtain the ( $|B_i|$ -dependent) relaxation rate for each noise:

$$\Gamma_1^{(i)} = \frac{1}{\hbar^2} |B_i|^2 S_i(\omega_{10}), \quad (2)$$

where  $\omega_{10}=(E_1-E_0)/\hbar$  and the power spectrum is defined by  $S_i(\omega) = \int_{-\infty}^{+\infty} dt \langle \lambda_i(t+\tau) \lambda_i(t) \rangle e^{-i\omega\tau}$ . The sum of all  $\Gamma_1^{(i)}$  gives the total relaxation rate  $\Gamma_1=1/T_1$ , where  $T_1$  is the relaxation time.

The longitudinal qubit-environment coupling introduces a random phase between the qubit eigenstates. At time  $\tau$  this random phase is  $\Delta\phi_i=(1/\hbar)\int_0^\tau dt X_i(t)$ . For a Gaussian noise, the dephasing factor  $\eta_i(\tau)$  is given by<sup>9</sup>  $e^{-\eta_i(\tau)} \equiv \langle e^{i\Delta\phi_i} \rangle = \exp[-\frac{1}{2}\langle (\Delta\phi_i)^2 \rangle]$ , where the brackets  $\langle \dots \rangle$  denote the quantum statistical average over the environment. Because  $X_i(t) = A_i \delta\lambda_i(t)$ , one can write the dephasing factor as

$$\eta_i(\tau) = \frac{1}{\hbar^2} |A_i|^2 \int_{\omega_c}^{+\infty} d\omega S_i(\omega) \frac{\sin^2(\omega\tau/2)}{2\pi(\omega/2)^2}, \quad (3)$$

where  $\omega_c$  is a low-frequency cutoff determined by the measurement time. The pure dephasing rate  $\Gamma_\varphi=1/T_\varphi$  is defined by  $\sum_i \eta_i(T_\varphi)=1$ . The dephasing factor  $\eta_i(\tau) \propto |A_i|^2$ , consistent

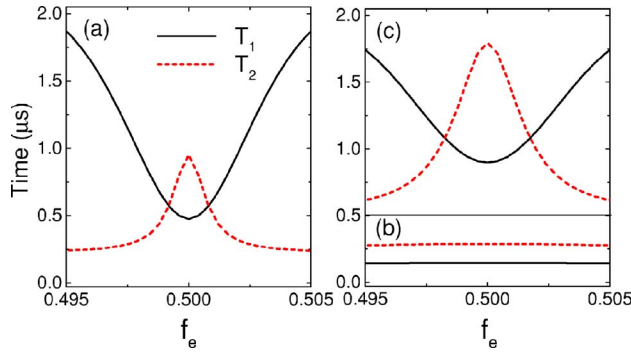


FIG. 4. (Color online) Relaxation and decoherence times ( $T_1$  and  $T_2$ ) for three flux qubits with the same noise sources. The parameters are  $E_J/E_C=35$ ,  $\alpha=\beta=(a)$  0.8, (b) 0.6, and (c)  $\alpha=0.6$ ,  $\beta=4$ . Here, as a simple estimation, we ignore the frequency dependence of the power spectra around  $f_e=0.5$  and determine their high- and low-frequency components via Eqs. (2) and (3) by assuming  $T_1=0.5 \mu\text{s}$  and  $T_2=0.8 \mu\text{s}$  at  $f_e=0.5004$  for the qubit in (a).

with reducing pure dephasing by decreasing the longitudinal coupling. Moreover, relaxation can also cause damping of the off-diagonal density matrix elements. Following the Bloch-Redfield theory (see, e.g., Ref. 12), the total damping of the off-diagonal elements is characterized by a decoherence rate  $\Gamma_2=1/T_2$ , with  $\Gamma_2=\frac{1}{2}\Gamma_1+\Gamma_\varphi$ .

In Fig. 4, we show  $T_1$  and  $T_2$  for three hypothetical flux qubits calculated using the same noise sources. The qubit in Fig. 4(a), with  $\alpha=\beta=0.8$ , is a conventional qubit with no shunt capacitance.<sup>3</sup> The qubits in Figs. 4(b) and 4(c) have a reduced value of  $\alpha$  (0.6 for both figures), and a shunt capacitor (with  $\beta=4$ ) is added for Fig. 4(c). As compared with the conventional qubit in Fig. 4(a), the decoherence time  $T_2$  in

Fig. 4(c) is larger by a factor of 2 at the degeneracy point and the  $T_2$  peak is broader. Furthermore, the qubit in Fig. 4(c) has a larger gap than the qubit in Fig. 4(a),  $\Delta \approx 0.02E_J$  compared to  $\Delta \approx 0.013E_J$ . Combining the increase in both  $T_2$  and  $\Delta$ , we find that the quality of quantum coherence is improved by a factor of 3 at the degeneracy point. Away from the degeneracy point (e.g., at  $f_e=0.4988$ ),  $T_2$  can be improved by a factor of 3 and the quality of coherence is improved by a factor of 5 (nearly one order of magnitude). Also, at  $f_e \sim 0.5$ ,  $T_2$  is reduced by about one order of magnitude if the shunt capacitor is removed [comparing Figs. 4(c) and 4(b)]. These results further show the important role of the shunt capacitance in achieving a low-decoherence flux qubit.

In conclusion, we have proposed a qubit design modified from the commonly used flux qubit. The qubit decoherence is reduced by shunting the small JJ with an additional capacitor. We show that by increasing the shunt capacitance and reducing the coupling energy of the JJ, the effects of both charge and flux noises are considerably suppressed. Recently, a shunt capacitor was used to improve the performance of phase qubits.<sup>13</sup> In that case the motivation for adding the shunt capacitor was quite different from ours; they used a smaller junction so as to reduce the number of two-level systems in the junction but decreased the charging energy of the junction with a shunt capacitor in order to push the qubit back into the phase regime. However, in our case the effects of the noise are suppressed even though we assume that the noise source remains unchanged.

We would like to thank M. Grajcar and A. M. Zagorskin for valuable discussions. This work was supported in part by the NSA, LPS, and ARO. J.Q.Y. was supported by NFRPC Grant No. 2006CB921205 and NSFC Grants Nos. 10474013, 10534060, and 10625416. S.A. was supported by the JSPS.

<sup>1</sup>J. Q. You and F. Nori, *Phys. Today* **58** (11), 42 (2005).

<sup>2</sup>T. P. Orlando, J. E. Mooij, L. Tian, C. H. van der Wal, L. Levitov, S. Lloyd, and J. J. Mazo, *Phys. Rev. B* **60**, 15398 (1999).

<sup>3</sup>I. Chiorescu *et al.*, *Science* **299**, 1869 (2003).

<sup>4</sup>J. Q. You, Y. Nakamura, and F. Nori, *Phys. Rev. B* **71**, 024532 (2005).

<sup>5</sup>E. Il'ichev, N. Oukhanski, A. Izmalkov, T. Wagner, M. Grajcar, H. G. Meyer, A. Y. Smirnov, A. Maassen van den Brink, M. H. S. Amin, and A. M. Zagorskin, *Phys. Rev. Lett.* **91**, 097906 (2003); M. Grajcar *et al.*, *ibid.* **96**, 047006 (2006).

<sup>6</sup>S. Saito, M. Thorwart, H. Tanaka, M. Ueda, H. Nakano, K. Semba, and H. Takayanagi, *Phys. Rev. Lett.* **93**, 037001 (2004); F. Yoshihara, K. Harrabi, A. O. Nishkanen, Y. Nakamura, and J. S. Tsai, *ibid.* **97**, 167001 (2006); B. L. T. Plourde, T. L. Robertson, P. A. Reichardt, T. Hime, S. Linzen, C. E. Wu, and J. Clarke, *Phys. Rev. B* **72**, 060506(R) (2005).

<sup>7</sup>P. Bertet, I. Chiorescu, G. Burkard, K. Semba, C. J. P. M. Harmans, D. P. DiVincenzo, and J. E. Mooij, *Phys. Rev. Lett.* **95**, 257002 (2005); arXiv:cond-mat/0412485 (unpublished) contains additional information.

<sup>8</sup>Y. X. Liu, L. F. Wei, J. S. Tsai, and F. Nori, *Phys. Rev. Lett.* **96**, 067003 (2006).

<sup>9</sup>Y. Nakamura, Y. A. Pashkin, T. Yamamoto, and J. S. Tsai, *Phys. Rev. Lett.* **88**, 047901 (2002).

<sup>10</sup>L. B. Ioffe, V. B. Geshkenbein, C. Helm, and G. Blatter, *Phys. Rev. Lett.* **93**, 057001 (2004).

<sup>11</sup>J. M. Martinis *et al.*, *Phys. Rev. Lett.* **95**, 210503 (2005).

<sup>12</sup>C. Cohen-Tannoudji *et al.*, *Atom-Photon Interaction* (Wiley, New York, 1992), Chap. 4.

<sup>13</sup>M. Steffen, M. Ansmann, R. McDermott, N. Katz, R. C. Bialczak, E. Lucero, M. Neeley, E. M. Weig, A. N. Cleland, and J. M. Martinis, *Phys. Rev. Lett.* **97**, 050502 (2006).